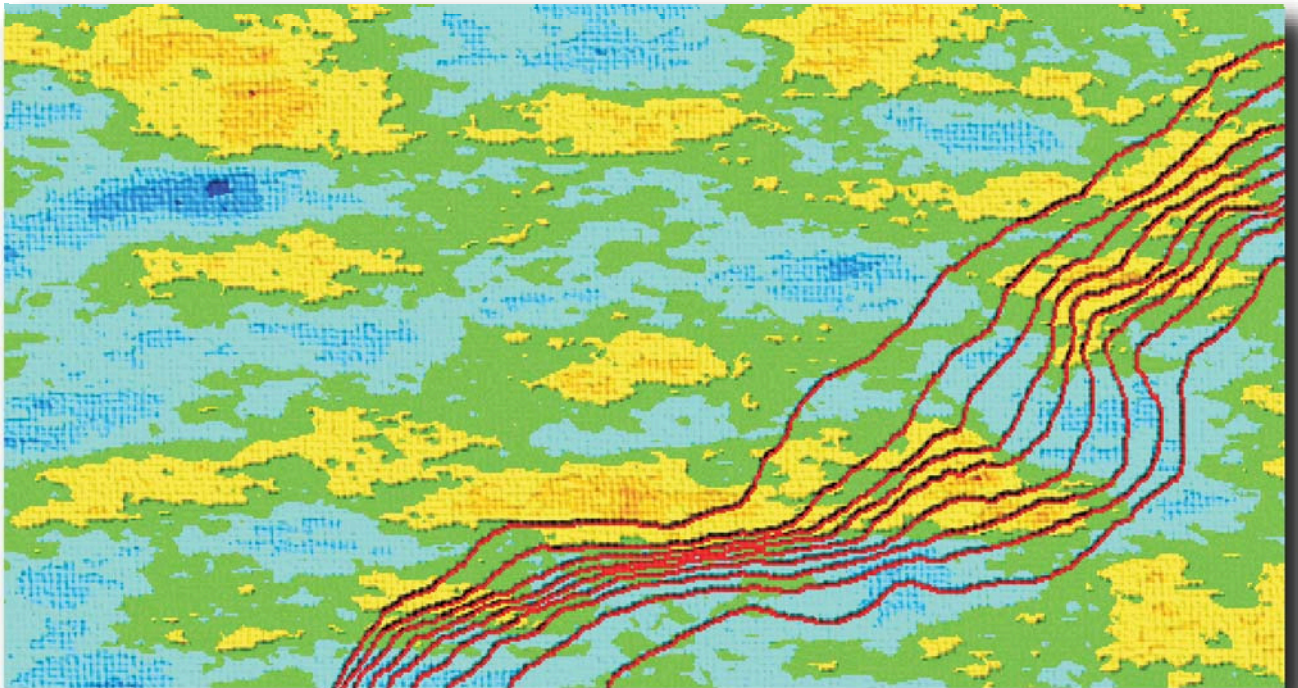


# SEAWATER INTRUSION IN COMPLEX GEOLOGICAL ENVIRONMENTS

Elena Abarca Cameo  
PhD Thesis



Supervisors:  
Xavier Sánchez-Vila  
Jesús Carrera



**Grup d'Hidrologia Subterrània**  
UNIVERSITAT POLITÈCNICA DE CATALUNYA





# SEAWATER INTRUSION IN COMPLEX GEOLOGICAL ENVIRONMENTS

PhD Thesis

Department of Geotechnical Engineering and Geo-Sciences (ETCG)

Technical University of Catalonia, UPC

Elena Abarca Cameo

March, 2006



**HYDROGEOLOGY GROUP**  
TECHNICAL UNIVERSITY OF CATALONIA

This thesis was funded by the Catalonia Government (GENCAT) with a FI grant and by the UPC with a grant to finish the PhD thesis and was developed in the framework of the European project SALTRANS, *Methods for assessing salt intrusion and transport in heterogeneous and fractured aquifers*, contract EVK1-CT-2000-00062.

*A mis padres, Eloy y Elena.*



# Abstract

Modelling seawater intrusion (SWI) has evolved from a tool for understanding to a water management need. Yet, it remains a challenge. Difficulties arise from the assessment of dispersion coefficients and the complexity of natural systems that results in complicated aquifer geometries and heterogeneity in the hydraulic parameters. Addressing such difficulties is the objective of this thesis. Specifically, factors that may affect the flow and transport in coastal aquifers and produce heterogeneous salinity distributions are studied.

First, a new paradigm for seawater intrusion is proposed since the current paradigm (the Henry problem) fails to properly reproduce observed SWI wedges. Mixing is represented by means of a velocity dependent dispersion tensor in the new proposed problem. Thereby, we denote it as "dispersive Henry problem". SWI is characterized in terms of the wedge penetration, width of the mixing zone and influx of seawater. The width of the mixing zone depends basically on dispersion, with longitudinal and transverse dispersion controlling different parts of the mixing zone but displaying similar overall effects. The wedge penetration is mainly controlled by the horizontal permeability and by the geometric mean of the dispersivity coefficients. Transverse dispersivity and the geometric mean of the hydraulic conductivity are the leading parameters controlling the amount of salt that enters the aquifer.

Second, the effect of heterogeneity was studied by incorporating heterogeneity in the hydraulic permeability into the modified Henry problem. Results show that heterogeneity causes the toe to



recede while increases both the width and slope of the mixing zone. The shape of the interface and the saltwater flux depends on the distribution of the permeability in each realization. However, the wedge penetration and the width of the mixing zone do not show large fluctuations. Both variables are satisfactorily reproduced, in cases of moderate heterogeneity, by homogeneous media with equivalent permeability and either local or effective dispersivities.

Third, the effect of aquifer geometry in horizontally large confined aquifers was analyzed. Lateral slope turned out to be a critical factor. Lateral slopes in the seaside boundary of more than 3% cause the development of horizontal convection cells. The deepest zones act as preferential zones for seawater to enter the aquifer and preferential discharging zones are developed in the upwards lateral margins. A dimensionless number,  $N_{by}$ , which compares the seawards driving force to the lateral component of buoyancy, has been defined to estimate the relative importance of this effect.

All these factors can be determinant to explain the evolution of salinity in aquifers such as the Main aquifer of the Llobregat delta. Finally, a management model of this aquifer is developed to optimally design corrective measures to restore the water quality of the aquifer. The application of two different optimization methodologies, a linear and a non-linear optimization method, allowed (1) to quantify the hydraulic efficiency of two potential corrective measures: two recharge ponds and a seawater intrusion barrier; (2) to determine the water necessary to be injected in each of these measures to restore the water quality of the aquifer while minimizing changes in the pumping regime and (3) to assess the sustainable pumping regime (with and without the implementation of additional measures) once the water quality has been restored. Shadow prices obtained from linear programming become a valuable tool to quantify the hydraulic efficiency of potential corrective measures.

# Resumen

La modelación de la intrusión marina ha pasado de ser una herramienta de conocimiento a convertirse en una necesidad para la gestión de acuíferos costeros. Sin embargo, dicha modelación continúa suponiendo un reto. Las dificultades provienen de la difícil evaluación de los coeficientes de dispersión y de la complejidad de los sistemas naturales que se traduce en la existencia de complicadas geometrías de los acuíferos y en la heterogeneidad en los parámetros hidráulicos. El objetivo de esta tesis es abordar estas dificultades y, más específicamente, los factores que pueden afectar al flujo y transporte en acuíferos costeros produciendo distribuciones heterogéneas de salinidad.

En primer lugar, se ha definido un nuevo paradigma para la intrusión marina, ya que el existente (el problema de Henry) no reproduce adecuadamente las cuñas de intrusión marina observadas. En el nuevo paradigma, la mezcla se representa por medio de un tensor de dispersión dependiente de la velocidad, por ello, se denomina 'problema de Henry dispersivo'. La intrusión marina se caracteriza por la penetración de la interfaz, el ancho de la zona de mezcla y el flujo de agua salada que entra en el acuífero. El ancho de la zona de mezcla depende, básicamente, de la dispersión. La dispersión transversal y longitudinal afectan a diferentes partes de la zona de mezcla aunque su efecto global es similar. La penetración de la cuña está controlada fundamentalmente por la permeabilidad horizontal y por la media geométrica de los coeficientes de dispersión. La dispersión transversal y la media geométrica de las permeabilidades son los parámetros que rigen la cantidad de agua salada que penetra en el acuífero.

En segundo lugar, se estudia el efecto en el problema de Henry dispersivo de la heterogeneidad en la conductividad hidráulica. Los resultados muestran que la heterogeneidad produce un retroceso de la penetración de la cuña, mientras aumenta en el ancho y la pendiente de la zona de mezcla. La forma de la interfaz y el flujo de agua salada son función de la distribución de las permeabilidades en cada realización. Sin embargo, los resultados de la penetración de la cuña y el ancho de la zona de mezcla no presentan grandes fluctuaciones. En caso de heterogeneidad moderada, ambas variables pueden ser reproducidas de forma satisfactoria por un medio homogéneo con dispersión local o efectiva.

En tercer lugar, se analiza el efecto de la geometría en acuíferos confinados de gran extensión horizontal. La pendiente lateral resulta ser un factor crítico. Pendientes laterales de más de un 3% inducen el desarrollo de celdas de convección horizontales. Las zonas más profundas actúan de zonas preferentes de entrada de agua salada mientras que las zonas preferentes de descarga se sitúan más cerca de los márgenes laterales, más someros. Para estimar la importancia relativa de este efecto, se define un número adimensional,  $N_{by}$ , que compara el empuje del agua dulce hacia el mar con la componente lateral de la flotación.

Todos estos factores pueden ser determinantes para explicar la evolución de la salinidad en acuíferos como el acuífero principal del delta del río Llobregat. Finalmente, se ha desarrollado un modelo de gestión para diseñar, de forma óptima, medidas correctoras para recuperar la calidad del agua de dicho acuífero. La aplicación de dos metodologías de optimización diferentes, una lineal y otra no lineal, ha permitido (1) cuantificar la eficiencia hidráulica de dos potenciales medidas correctoras: dos balsas de recarga artificial y una barrera contra la intrusión marina; (2) determinar el caudal de agua a inyectar en cada una de las medidas correctoras para restaurar la calidad del agua del acuífero procurando minimizar los cambios con respecto al régimen de bombeo actual y (3) evaluar el régimen de explotación sostenible, con y sin medidas correctoras, una vez que la calidad del acuífero se haya recuperado. Los precios sombra obtenidos de la programación lineal resultan una valiosa herramienta para cuantificar la eficiencia hidráulica de las medidas propuestas.

# Resum

La modelització de la intrusió marina ha passat de ser una eina de coneixement a convertir-se en una necessitat per a la gestió d'aqüífers costaners. Malgrat això, aquesta modelització continua suposant un repte. Les dificultats provenen de la difícil avaluació dels coeficients de dispersió i de la complexitat dels sistemes naturals que es tradueix en l'existència de complicades geometries dels aquífers i en l'heterogeneïtat en els paràmetres hidràulics. L'objectiu d'aquesta tesi és l'abordar aquestes dificultats i, més específicament, els factors que poden afectar al flux i transport en aquífers costaners produint distribucions heterogènies de salinitat.

En primer lloc, s'ha definit un nou paradigma per a la intrusió marina, ja que l'existent (el problema d'Henry) no reproduceix adequadament els tascons de intrusió marina observades. En el nou paradigma, la barreja es representa per mitjà d'un tensor de dispersió depenent de la velocitat, per això, es denomina 'problema de Henry dispersiu'. La intrusió marina es caracteritza per la penetració de la interfície, l'ample de la zona de barreja i el flux d'aigua salada que entra en l'aquífer. L'ample de la zona de barreja depèn, bàsicament, de la dispersió. La dispersió transversal i longitudinal afecten a diferents parts de la zona de barreja encara que el seu efecte global és similar. La penetració del tascó està controlada fonamentalment per la permeabilitat horitzontal i per la mitjana geomètrica dels coeficients de dispersió. La dispersió transversal i la mitjana geomètrica de les permeabilitats són els paràmetres que regeixen la quantitat d'aigua salada que penetra en l'aquífer.

En segon lloc, s'estudia l'efecte en el problema de Henry dispersiu de l'heterogeneïtat en la conductivitat hidràulica. Els resultats mostren que l'heterogeneïtat produeix una reculada de la penetració del tascó, mentre augmenta l'ample i el pendent de la zona de barreja. La forma de la interfície i el flux d'aigua salada és funció de la distribució de les permeabilitats en cada realització. No obstant això, els resultats de la penetració del tascó i l'ample de la zona de barreja no presenten grans fluctuacions. En cas d'heterogeneïtat moderada, ambdues variables poden ser reproduïdes de forma satisfactòria per un medi homogeni amb dispersió local o efectiva.

En tercer lloc, s'analitza l'efecte de la geometria en aqüífers confinats de gran extensió horitzontal. El pendent lateral resulta ser un factor crític. Pendents laterals de més d'un 3% induïxen el desenvolupament de cel·les de convecció horitzontals. Les zones més profundes actuen de zones preferents d'entrada d'aigua salada mentre les zones preferents de descàrrega se situen més prop del marge lateral, més succints. Per a estimar la importància relativa d'aquest efecte, es defineix un nombre adimensional,  $N_{by}$ , que compara l'embranchada de l'aigua dolça cap al mar amb la component lateral de la flotació.

Tots aquests factors poden ser determinants per a explicar l'evolució de la salinitat en aqüífers com l'aqüífer principal del delta del Llobregat. Finalment, s'ha desenvolupat un model de gestió per a dissenyar, de forma òptima, mesures correctores per a recuperar la qualitat de l'aigua de d'aquest aqüífer. L'aplicació de dues metodologies d'optimització diferents, una lineal i una altra no lineal, ha permès (1) quantificar l'eficiència hidràulica de dues potencials mesures correctores: dues basses de recàrrega artificial i una barrera contra la intrusió marina; (2) determinar el cabal d'aigua a injectar en cadascuna d'aquestes mesures per a restaurar la qualitat de l'aigua de l'aqüífer procurant minimitzar els canvis pel que fa al règim de bombament actual i (3) avaluar el règim d'exploració sostenible, amb i sense mesures correctores, una vegada que la qualitat de l'aqüífer s'hagi recuperat. Els preus ombra obtinguts de la programació lineal resulten una valuosa eina per a quantificar l'eficiència hidràulica de les mesures correctores proposades.

# Agradecimientos

Les agradezco en primer lugar a mis directores de tesis, Jesús Carrera y Xavier Sánchez-Vila, por darme la oportunidad de trabajar en diversos proyectos de investigación, por su apoyo, orientación y ayuda en el desarrollo de este trabajo. Jesús, gracias por tu generosidad. Muchas gracias a Enric Vázquez-Súñe por su valiosa ayuda y apoyo, en particular al comienzo. Gracias a Cliff Voss, por la oportunidad de trabajar con él y aportar otra manera de hacer las cosas.

Gracias a todos los compañeros de Grupo de Higrgeología del Departamento de Ingeniería del Terreno, Cartográfica y Geofísica de la UPC, por su amistad y por la agradable atmósfera diaria.

Gracias a todos los amigos que han compartido conmigo estos años con sus buenos y malos momentos. Gracias por su amistad y por sus ánimos. Gracias Juan, por aguantar berrinches, nervios e histerias. Por supuesto, quisiera agradecer el apoyo de mi familia, por estar siempre ahí y animarme a llegar siempre a donde quiera. También quiero agradecerles su paciencia infinita por soportar las cada vez más frecuentes ausencias.



# Table of Contents

<b>1</b>	<b>Introduction</b>	<b>1</b>
<b>2</b>	<b>Anisotropic Dispersive Henry Problem</b>	<b>9</b>
2.1	The Henry Problem . . . . .	10
2.2	Limitations of the Henry problem . . . . .	14
2.3	Methodology . . . . .	17
2.3.1	Problem definition . . . . .	17
2.3.2	Dimensionless form of the governing equations . . . . .	19
2.3.3	Case definition . . . . .	22
2.3.4	Numerical analysis . . . . .	23
2.3.5	Variables of interest . . . . .	24
2.4	Results . . . . .	25
2.4.1	Diffusive versus dispersive Henry problem . . . . .	25
2.4.2	Limitations of the dispersive Henry problem . . . . .	28
2.4.3	Sensitivity to the dimensionless parameters . . . . .	29
2.5	Discussion and conclusions . . . . .	37
<b>3</b>	<b>Seawater intrusion through heterogeneous aquifers</b>	<b>41</b>
3.1	Introduction . . . . .	41
3.1.1	Scope and objectives . . . . .	43
3.2	Methodology . . . . .	43
3.2.1	Study of the effect of heterogeneity in Seawater Intrusion . . . . .	44
3.2.2	Are there any effective parameters for flow and transport? . . . . .	45
3.3	Qualitative effect of heterogeneity in seawater intrusion . . . . .	49



3.4	Small scale heterogeneity . . . . .	52
3.4.1	Medium variance ( $\sigma^2 = 1$ ) . . . . .	52
3.4.2	Large variance ( $\sigma^2 = 2$ ) . . . . .	58
3.5	Medium scale heterogeneity . . . . .	61
3.5.1	Medium variance ( $\sigma^2 = 1$ ) . . . . .	62
3.5.2	Large variance ( $\sigma^2 = 2$ ) . . . . .	66
3.6	Effects on characteristic output variables . . . . .	67
3.7	Discussion and conclusions . . . . .	70
<b>4</b>	<b>Quasi-horizontal circulation cells in seawater intrusion</b>	<b>73</b>
4.1	Governing equations and dimensionless numbers . . . . .	77
4.1.1	Flow equation . . . . .	77
4.1.2	Transport equation . . . . .	79
4.1.3	Dimensionless Numbers . . . . .	79
4.2	Numerical modelling methodology . . . . .	81
4.3	Results . . . . .	84
4.3.1	Aquifers without lateral slope . . . . .	85
4.3.2	Lateral sloping aquifers . . . . .	85
4.4	Sensitivity analysis . . . . .	90
4.4.1	Dispersivity . . . . .	91
4.4.2	Freshwater boundary inflow . . . . .	91
4.4.3	Aquifer Thickness . . . . .	92
4.5	Conclusions . . . . .	93
<b>5</b>	<b>Optimal design of measures to correct seawater intrusion</b>	<b>95</b>
5.1	Methodology . . . . .	98
5.1.1	Linear optimization problem . . . . .	99
5.1.2	Non-linear optimization problem . . . . .	101
5.2	CASE STUDY: Application to the Llobregat Delta Main aquifer . . . . .	102
5.2.1	Background and problem statement . . . . .	102
5.2.2	Groundwater flow and solute transport model construction and calibration	105
5.2.3	Definition of a reference scenario . . . . .	107

---

5.2.4	Management model . . . . .	109
5.2.5	Linear optimization problem . . . . .	111
5.2.6	Non-linear optimization problem . . . . .	117
5.2.7	Comparison of results . . . . .	120
5.3	Conclusions . . . . .	124
<b>6</b>	<b>Conclusions</b>	<b>127</b>
<b>A</b>	<b>Apendix A: Tilted Ghyben-Herzberg Approximation</b>	<b>133</b>
A.1	V-shaped Aquifers . . . . .	134
A.2	Warped Aquifers . . . . .	135



# List of Figures

2.1	Henry problem domain and boundary conditions . . . . .	11
2.2	Real vertical electrical conductivity profiles and vertical salinity profiles in different aquifer formations . . . . .	16
2.3	Schematic description of the variables used to quantify seawater intrusion . . . . .	25
2.4	Diffusive seawater-freshwater mixing zone <i>versus</i> a purely dispersive mixing zone	26
2.5	Diffusive and dispersive vertical salinity profiles from numerical simulations . . . . .	27
2.6	Change in the interface shape and location with increasing diffusion and dispersion	27
2.7	Equivalent freshwater heads and concentration distributions for the uncoupled and coupled dispersive Henry problem . . . . .	28
2.8	Regressions obtained for the deviation of the toe penetration with respect to the Ghyben-Herzberg toe position . . . . .	31
2.9	Width of the mixing zone versus $x$ in the diffusive and dispersive reference cases	32
2.10	Velocity field and 25, 50 and 75% concentration isolines in the dispersive reference case. . . . .	33
2.11	Linear relationship of the width of the mixing zone with respect to the geometric mean of the dispersivity coefficients . . . . .	34
2.12	Concentration distribution for different simulations showing the effect of increasing independently the longitudinal and the transversal dispersion coefficient . . . . .	35
2.13	Regressions obtained for the dimensionless saltwater flux for the dispersive (left) and diffusive (right) case . . . . .	36
2.14	Qualitative summary of the behavior of the solution to the dispersive Henry problem	38
3.1	Scheme of numerical set-ups to obtain $K_{Heq}$ and $K_{Veq}$ . . . . .	46

3.2	Longitudinal and transverse effective dispersivity obtained by means of the perturbation theory ( <i>Dentz et al., 2000</i> ) for short correlation distances ( $\lambda_x = 0.045$ and $\lambda_y = 0.015$ ) . . . . .	48
3.3	Longitudinal and transverse effective dispersivity obtained by means of the perturbation theory ( <i>Dentz et al., 2000</i> ) for medium correlation distances ( $\lambda_x = 0.15$ and $\lambda_y = 0.045$ ) . . . . .	48
3.4	Freshwater/saltwater mixing zones in some heterogeneous media with with $\lambda_{medium}$ and $\sigma^2 = 1$ and $\sigma^2 = 2$ . . . . .	50
3.5	Comparison between the freshwater/saltwater mixing zone in an homogenous and a heterogeneous medium with the same effective permeability and plot vertically integrated flux along the seaside boundary ( $\int_0^z q_z dz$ ) . . . . .	51
3.6	Freshwater/saltwater mixing zones in some heterogeneous media with with short $\lambda$ and $\sigma^2 = 1$ . . . . .	53
3.7	Dispersive solution of two heterogeneous realizations with short $\lambda$ and $\sigma^2 = 1$ (dashed lines) compared to the solution of three different homogeneous media . .	55
3.8	Diffusive solution of two heterogeneous realizations with short $\lambda$ and $\sigma^2 = 1$ (dashed lines) compared to the solution of three different homogeneous media . .	56
3.9	Ensemble of concentrations of the 50 heterogeneous realizations with short $\lambda$ and $\sigma^2 = 1$ (dashed lines) for the dispersive and diffusive case compared to the solution of a homogeneous medium with $K_{eff}$ and local dispersion/diffusion . . . . .	57
3.10	Ensemble of concentrations of the 50 heterogeneous realizations with short $\lambda$ and $\sigma^2 = 1$ (dashed lines) for the dispersive case compared to the solution of a homogeneous medium with $K_{eff}$ and (1) effective dispersion coefficients or (2) macrodispersion . . . . .	57
3.11	Freshwater/saltwater mixing zones in some heterogeneous media with short $\lambda$ and $\sigma^2 = 2$ . . . . .	59
3.12	Isoconcentration lines for two heterogeneous realizations with short $\lambda$ and $\sigma^2 = 2$ (dashed lines) compared to a medium two homogeneous medium, one with local and the other with effective dispersivity coefficients. . . . .	60
3.13	Diffusive interface (dashed lines) for two heterogeneous realizations with short $\lambda$ and $\sigma^2 = 2$ compared to an homogenous medium with the local diffusion coefficient. . . . .	61
3.14	Dispersive solution of two heterogeneous realizations with medium $\lambda$ and $\sigma^2 = 1$ (dashed lines) compared to the solution of three different homogeneous media . .	63

3.15	Diffusive solution of two heterogeneous realizations medium $\lambda$ and $\sigma^2 = 1$ (dashed lines) compared to the solution of three different homogeneous media . . . . .	64
3.16	Ensemble of concentrations of the 50 heterogeneous realizations with medium $\lambda$ and $\sigma^2 = 1$ (dashed lines) for the dispersive and diffusive case compared to the solution of a homogeneous medium with $K_{eff}$ and local dispersion/diffusion . . . . .	65
3.17	Ensemble of concentrations of the 50 heterogeneous realizations with short $\lambda$ and $\sigma^2 = 1$ (dashed lines) for the dispersive case compared to the solution of a homogeneous medium with $K_{eff}$ and (1) effective dispersion coefficients or (2) macrodispersion . . . . .	65
3.18	Diffusive interface (dashed lines) for two heterogeneous realizations (medium $\lambda$ and $\sigma^2 = 2$ ) compared to an homogenous medium with the local diffusion coefficient. . . . .	66
3.19	Isoconcentration lines for two heterogeneous realizations with medium $\lambda$ and $\sigma^2 = 2$ (dashed lines) compared to a medium two homogeneous medium, one with local and the other with effective dispersivity coefficients. . . . .	67
3.20	Box-plots showing the distribution of the results of $L_D$ , $W_D$ and $R_D$ for the 50 random realizations of each series, their homogeneous media and the ensemble average of concentrations . . . . .	68
3.21	Comparison of the ensembles of the heterogeneous media with small correlation length (dashed lines) and with medium correlation length (solid line). . . . .	70
4.1	Classical vertical saltwater circulation cell induced by the combination of buoyancy forces and hydrodynamic dispersion processes. . . . .	74
4.2	Geometry of the aquifer and model domain, including boundary conditions . . . . .	81
4.3	Schematic description of the test cases geometries: (1) horizontal, (2) seawards sloping, (3) V-shaped and (4) warped . . . . .	82
4.4	Interface position in the central cross section for seawards sloping and warped aquifers . . . . .	85
4.5	Velocity vectors on the aquifer central cross section projected in the XZ plane . . . . .	86
4.6	Velocity vectors at the aquifer bottom projected in the XY plane, isoconcentration lines and equivalent freshwater head isolines in a V-shaped and warped aquifer with $N_{by}=2.0$ . . . . .	87
4.7	Toe position for the central cross section and the lateral cross section . . . . .	88
4.8	Vertically integrated salt flux per unit length of coastline . . . . .	89
4.9	Model results at the bottom of the V-shaped and warped aquifers with $N_{by} = 2.0$ . . . . .	90

4.10	Sensitivity of toe penetration in the aquifer central cross section to the longitudinal (left) and transversal (right) dispersivity values for different aquifer geometries. . . . .	91
4.11	Sensitivity of toe penetration in the aquifer central cross section to the freshwater inflow through the inland boundary for different aquifer geometries. . . . .	92
4.12	Sensitivity of toe penetration in the aquifer central cross section to different aquifer thickness for the different considered aquifer geometries. . . . .	93
5.1	Location of the Llobregat delta and lower valley . . . . .	103
5.2	Modified from <i>Simó et al.</i> (2005). Geological cross section perpendicular to the coast of the emerged and submerged Llobregat delta . . . . .	104
5.3	Modified from <i>Simó et al.</i> (2005). Paleochannel systems (A, B, C) associated to the main aquifer of the Llobregat delta . . . . .	104
5.4	Piezometric map calculated for December 2001 together with the heads mean error and the calculated versus measured heads at four observation points . . . . .	107
5.5	Chloride concentration map calculated for December 2001 together with the concentration mean error and the calculated versus measured chloride concentration at six observation points . . . . .	108
5.6	Location of the pumping wells and their average pumping rate in the period from 1997 to 2001 and location of the proposed corrective measures . . . . .	109
5.7	(a) Management areas defined in the aquifer according to geological, hydrological and management criteria and (b) location of the control points used for the optimization process . . . . .	110
5.8	Results of the optimization of pumping rates for every management area and the total value of the objective function for different flow constraints applied . . . . .	113
5.9	Results of the optimization with additional corrective measures of pumping rates for every management area and the total value of the objective function for different flow constraints applied . . . . .	114
5.10	Chloride concentration map in the main aquifer of the Llobregat Lower Valley obtained (a) form the linearly optimized pumping rates and the implementation of corrective measures and (b) for the reference scenario . . . . .	116
5.11	Results of the non-linear optimization problem. Obtained pumping rates per management zones and measures (gray bars) are compared to current values or projected values in the case of corrective measures (white bars). . . . .	119

---

5.12 Chloride concentration map in the main aquifer of the Llobregat Lower Valley obtained (a) from the non-linearly optimized pumping rates and the implementation of corrective measures and (b) for the reference scenario . . . . .	120
A.1 Plan view of the aquifer domain and some of the variables that appear in the calculations of the tilted Ghyben-Herzberg approximation . . . . .	134





# List of Tables

2.1	Original parameters used in Henry problem . . . . .	12
2.2	Dimensionless parameters for reference cases . . . . .	22
2.3	Number of elements used depending in the shape factor $\xi$ . . . . .	24
3.1	Geostatistical description of all cases studied (lengths are scaled by the aquifer thickness) . . . . .	44
4.1	Parameters used in the simulations . . . . .	83
4.2	Description of simulations considered in the analysis ( $m_x$ and $m_y$ are the components of the slope perpendicular and parallel to the sea coast, respectively) . . . . .	83
5.1	Statistical parameters used in the simulations . . . . .	118
5.2	Comparison of the results obtained with the linear (LOP) and non-linear optimization process (NLOP) for the more realistic optimization scenarios (values in $hm^3/y$ )	121
5.3	Comparison of the two methods considered in this paper . . . . .	122



# Chapter 1

## Introduction

Below the discharging freshwater in coastal aquifers, there exists a saltwater wedge formed by recirculating seawater. This wedge develops due to both density driven flow and hydrodynamic dispersion. Intensive groundwater abstraction alters the equilibrium between freshwater and saltwater with the net result of an inland movement of the wedge (seawater intrusion) and upward movement of saltwater below partially penetrating pumping wells (upconing).

Seawater intrusion is a common contamination problem in coastal areas. It affects, mainly, arid and semi-arid zones, where dense population and touristic development are coupled to scarce water resources and require intense exploitation of groundwater (particularly in the dry season). The Mediterranean coast is a clear example (*El-Bihery and Lachmar, 1994; Bonacci and RojeBonacci, 1997; Chiocchini et al., 1997; Yakirevich et al., 1998; Pulido-Bosch et al., 1999; Petalas and Diamantis, 1999; Paniconi et al., 2001b; Arfib and de Marsily, 2004*), and the Spanish littoral is not an exception (*Iribar, 1992; Calvache and Pulido-Bosc, 1994; Barón et al., 1994; Gimenez and Morell, 1997; Padilla et al., 1997; Pulido-Leboeuf, 2004*). Due to its socioeconomic impact, this issue has received an ample attention from the international scientific community during the last 40 years (*Cooper, 1964; Henry, 1964; Pinder and Cooper, 1970; Custodio and Bruggeman, 1987;*

*Falkland, 1991; Xue et al., 1995; Bear and et al., 1999; Cheng et al., 2001; Barlow, 2003; Zhang et al., 2004; Post, 2004; Prieto, 2005).*

Despite the large amount of scientific literature about this topic, many questions remain open (*Simmons et al., 2001; Diersch and Kolditz, 2002; Simmons, 2005*). Uncertain remains the effect of some natural factors such as: tidal effects, three-dimensionality, heterogeneity, transient variations of the freshwater recharge and unsaturated effects. Some of this factors have been subject of recent studies. *Thorenz et al. (2002)* experimentally and numerically studied the interaction of fresh and saltwater in the partially saturated regions above the water table. *Prieto (2005)* studied the influence of periodic tidal fluctuations in the seawater intrusion behavior. Addressing the effect of some of these factor is the objective of this thesis. Specifically, factors that may affect the flow and transport in coastal aquifers and produce heterogeneous salinity distributions are studied.

One of the paradigms to understand seawater intrusion is the well-known Henry problem (*Henry, 1964*). However, this problem displays some limitations to realistically represent the salt-water wedges. First, it considers mixing as a result of constant diffusion and second, the diffusion coefficient applied is too high. The resulting intrusion wedge presents a shape and width of the mixing zone that does not resemble field observations. Therefore, the first objective of this thesis is to define a more realistic paradigm to represent seawater intrusion. This paradigm must provide insights into the factors governing the seawater intrusion wedge at steady state, in particular, the effect of dispersivity and anisotropy in the hydraulic conductivity.

Most of the existing seawater intrusion studies consider homogeneous media. However, heterogeneity is of extreme importance in many coastal deposits as in deltaic aquifers where lateral variations of facies are frequent and there exist paleochannels that act as preferential paths for incoming seawater. Heterogeneity is known to produce dispersion (*Dagan, 1989; Dentz et al., 2000; Dentz and Carrera, 2003; Cirpka and Attinger, 2003*) and, therefore, it is susceptible of affecting the seawater intrusion wedge. The second specific objective of this thesis that is to determine the effect of heterogeneity in the hydraulic conductivity on the dynamics of the seawater intrusion.

Classical seawater intrusion studies looked at 2D vertical cross sections. It is known that the seawater wedge penetration depends on the depth of the aquifer bottom. Variation in the depth of the aquifer bottom are non unusual in coastal aquifers, e.g., in deltaic aquifers, the central part is usually deeper than the margins of the aquifer. Geophysical studies provide evidence that seawater penetrates further inland at the deepest portion of coastal aquifers (*Flores-Márquez et al.*, 1998; *Rangel-Medina et al.*, 2003; *Benkabbour et al.*, 2004). However, the effect of the three-dimensional topography of the basement in the seawater intrusion in confined aquifers has not been systematically analyzed. Thereby, the third objective of this thesis is to evaluate the effect of aquifer shape on seawater intrusion.

Finally, a high degree of complexity, that of a real aquifer, is considered. In particular, a model of a hydrogeologically complex aquifer, the main aquifer of the Llobregat delta, is performed. This aquifer motivates many of the questions addressed in this thesis, since it is a heterogeneous aquifer with lateral variations of bottom topography. This confined aquifer is ideal for studying seawater intrusion because, first, it has been affected by seawater intrusion for many decades; second, seawater intrusion shows a complex evolution in space and time; third, there is a large amount of available head and chloride data; and fourth, it has a strategic importance for supply purposes under scarcity to the Barcelona metropolitan area.

For this last reason, there is a need for the recovery of the water quality of the Llobregat delta aquifers, which has kept Water Agencies actively involved in their management. As a result, the main aquifer has received increasing attention since the 60's (*MOP*, 1966; *Custodio et al.*, 1976; *Bayó et al.*, 1977; *Custodio*, 1981; *PHPO*, 1985; *Custodio et al.*, 1989; *Iribar*, 1992; *Manzano et al.*, 1992). Huge abstraction during the 70's for industrial purposes caused an important piezometric depression that reached values below -25 m.a.s.l. However, although drawdown was generalized in all the aquifer extension, salinization occurred following a spatially irregular pattern (*Iribar and Custodio*, 1992). Preferential pathways for incoming seawater (fingers) were observed around freshwater areas. Although the absolute values of salinity have changed with time, this

spatially heterogeneous salinity distribution is still present nowadays. Seawater evolution in this aquifer illustrate that seawater intrusion is very sensitive to factors such as the aquifer geometry and the heterogeneity of hydraulic properties. Heterogeneity in coastal aquifers conditions the location of pathways for saltwater, and the nature and shape of the interface between fresh and salt water.

Various existing groundwater flow models of this aquifer adequately reproduce piezometric heads (*Cuena and Custodio, 1971; Custodio et al., 1971; PHPO, 1985; Iribar et al., 1997*). However, efforts delivered to jointly represent the piezometric and salinity evolution have not been, up to date, so satisfactory (*Iribar, 1992*). To efficiently manage an aquifer of such characteristics, a reliable numerical model that can realistically quantify the water inputs and outputs and that can be used to evaluate seawater intrusion evolution under a wide variety of management scenarios is needed. Those models are also crucial to design corrective measures and remediation strategies. The development of such a model was part of the objectives of the project “*Programa de gestió dels aqüífers de la Cubeta de Sant Andreu, Vall Baixa i delta del Llobregat*”, funded by *L’agència catalana de l’aigua* (Catalonian Water Agency) and the SALTRANS European project (EVK1-CT-2000-00062), in the framework of which this thesis was developed. The main objective of the latter was to develop a methodology for assessment of groundwater contamination in heterogeneous aquifers, as a result of intrusion and transport of salts and saline water. The fourth specific objective of this thesis, integrated in this framework, is to integrate the acquired insights into the Llobregat delta main aquifer and into its water resources management.

In summary, a numerical analysis of seawater intrusion in increasingly complex systems is carried out. This thesis is structured to tackle seawater problems related to an increasing degree of complexity. The general objective of this thesis is to advance in the knowledge of the hydrodynamic processes that take place in coastal aquifers and control the evolution and development of seawater intrusion. Basically, the aim is to understand the effect of geometry, dispersion and heterogeneity in hydraulic conductivity on the position of the saltwater-freshwater interface. Their

combined effect can act in a synergistic way to significantly affect the seawater intrusion behavior.

## Thesis outline

This thesis consists of five chapters after the introductory one. Except for the last one, each chapter responds to one of the above mentioned specific objectives. Those chapters are based on papers that are being or have been submitted to international journals and are being under review. The reference to the papers is indicated in a footnote at the beginning of each chapter.

Chapter 2 proposes a modification of Henry original problem, still considering a homogeneous aquifer. The aim is to ensure, first, sensitivity to density variations and, second, vertical salinity profiles that resemble field observations. In this problem, mixing is represented by means of the traditional Scheidegger dispersion tensor (dispersivity times water flux) instead of a groundwater velocity independent diffusion coefficient. Thus, we denote it as "dispersive Henry problem". Moreover, anisotropy in the hydraulic conductivity is acknowledged and Henry's seaside boundary condition of prescribed salt concentration is substituted by a flux dependent boundary condition, which represents more realistically salt transport across the seaside boundary.

Chapter 3 focusses on the importance of integrating natural heterogeneity in seawater intrusion modelling. Real aquifers are heterogeneous, yet most models describing saltwater intrusion into coastal aquifers do not take into account spatial heterogeneity of hydraulic conductivity. The questions addressed in this chapter are: (1) whether a heterogeneous medium can ever be represented by a homogeneous effective medium, (2) can we find a first approximation to the effective parameters that should be used and what is the information lost in this process. To this end, heterogeneity in hydraulic conductivity has been applied to the modified Henry problem presented in Chapter 2, in both its diffusive and dispersive forms. It is well established that dispersion is enhanced by spatial heterogeneity. Therefore, one of the main objectives of this study is to assess the effect of spatial variability of hydraulic conductivity on equivalent dispersivity, since this is a most



significant and difficult parameter to assess in seawater intrusion models. Spatial heterogeneity is analyzed within a geostatistical framework using a methodology based on Monte Carlo analysis. The basic steps are: first, a geostatistical model is selected and a number of heterogeneous hydraulic conductivity fields are generated for each model. Second, Henry's problem is solved for all heterogeneous fields. Specifically, we aim at finding appropriate equivalent values for the hydraulic permeability and dispersivity as a function of heterogeneity.

Chapter 4 studies the effect of the variations in the aquifer bottom topography over the seawater-freshwater interface. The analysis is carried out in steady state, in aquifers with large horizontal extent compared to their thickness. In these cases, while buoyancy acts in the vertical direction, flow is confined between the upper and bottom boundaries and the effect of gravity is controlled by variations in aquifer elevation. Therefore, the effective gravity is controlled by the slope and shape of the aquifer. Variability in the topography of the aquifer boundaries is one case where three-dimensional analysis is necessary. In this work density dependent flow processes caused by the three-dimensionality of the aquifer geometry are studied numerically and the analysis concentrates on the lateral slope of the aquifer.

Chapter 5 presents part of an extensive work carried out by a group of people in the framework of two projects: the SALTRANS project and a project with the Catalonia Water Agency (*L'Agència Catalana de l'Aigua*) for the development of a management model of the Lower Valley and delta of the Llobregat River. The entire work is included in the several reports written for the Catalonia Water Agency. Part of this work has been already presented in some national and international meetings, and the most novel aspects have been the subject of papers that have been submitted to international journals. One of these papers is presented in this chapter. It focusses on the optimization of management strategies in the Llobregat delta aquifers, that correspond to the latest step of the project.

In this chapter the use of two different optimization methodologies to assess management strategies in coastal aquifers is proposed. Little has been done in the numerous studies of op-

timization of groundwater resources to address the restoration of aquifers initially affected by seawater intrusion, which is the objective of this paper. To this end, we compare two optimization methods applied to control seawater intrusion in the main aquifer of the Llobregat delta. The first one is linear and consists of maximizing pumping rates while constraining heads to prevent seawater inflow. The second one consists of minimizing the variation from current pumping rates, so as to preserve existing rights, while constraining concentrations. This leads to a non-linear programming problem. In both cases, corrective measures include potential reduction of pumping rates, inland artificial recharge and a coastal hydraulic barrier.

A last chapter summarizes the main contributions of this thesis.



## Chapter 2

# Anisotropic Dispersive Henry Problem\*

Most density dependent flow benchmark problems represent unstable systems with buoyancy acting as the driving force, resulting in fingering and convection cells. A classical test is the Elder Problem (Elder, 1967), which has been questioned because of the dependence of results on grid refinement (Frolkovic and De Schepper, 2000; Woods et al., 2003) and the non-uniqueness of the solution (Johannsen, 2003). Other tests involve comparing code results for a proposed problem (OECD, 1988). In those cases, the problem has to be extremely well defined or the differences in the results may be mainly caused by the different conceptualization of the problem (Konikow et al., 1997) rather than by code discrepancies. There is a demand for reliable density driven flow tests, and new benchmark problems have been proposed during recent years. Recent proposals for benchmark problems include carefully monitored laboratory experiments such as the Salt Lake problem (Simmons and Wooding, 1999) or, more recently, the Salt Pool problem (Oswald and Kinzelbach, 2004; Johannsen et al., 2002). Weatherill et al. (2004) proposed as benchmark tests three variations of the Horton-Rogers-Lapwood problem: the "infinite horizontal box", "finite horizontal box" and "infinite inclined box". These problems are characterized by well defined sta-

---

\*This chapter is based on the paper: Abarca, E., Carrera, J., Sanchez-Vila, X. and Dentz, M., submitted to *Adv. in water resour.*, Anisotropic Dispersive Henry Problem

bility indicators (the critical Rayleigh number and a convective wavelength) that can be determined analytically. Unfortunately, none of these benchmarks reproduce the boundary conditions encountered in typical seawater intrusion problems. For years, this role has been reserved to the Henry problem.

## 2.1 The Henry Problem

Seawater intrusion into coastal aquifers exemplifies natural stable density stratification with denser saltwater encroaching below freshwater. An abstraction of the saltwater intrusion problem in a vertical cross-section perpendicular to the coast line was introduced by Henry (*Henry*, 1964). The solution achieved its objective, as it helped in shaping the basic hydraulic concepts of seawater intrusion as we understand them nowadays. The conceptual model is that of a confined aquifer with homogeneous isotropic hydraulic conductivity, and the boundary conditions (BC) of Figure 2.1: no-flow along the top and bottom boundary, specified freshwater seepage along the inland boundary and prescribed saltwater hydrostatic pressure along the seaside boundary. The original Henry problem considers advection and diffusion (no dispersion). This configuration leads to a characteristic, stationary saltwater intrusion wedge penetrating landward on the aquifer bottom. *Henry* (1964) provided a semi-analytical solution for this problem configuration. His solution was revised and improved by *Borisov et al.* (1996) and *Segol* (1994). The semi-analytical solution in those studies was given as an infinite-series solution. More recently, *Dentz et al.* (2005) proposed a perturbation method solution to this problem. The Henry problem solution depends on three dimensionless parameters:

$$a = \frac{q_b}{K\epsilon} \quad b = \frac{D_m\phi}{q_b d} \quad \xi = \frac{L}{d} \quad (2.1)$$

where  $q_b$  is freshwater recharge rate,  $K$  hydraulic conductivity,  $\epsilon$  density contrast parameter,  $D_m$  molecular diffusion coefficient,  $\phi$  porosity,  $d$  aquifer thickness and  $L$  aquifer length.  $a$  com-

pares viscous ( $q_b/K$ ) and buoyancy ( $\epsilon$ ) forces and will be termed dimensionless freshwater flux.  $b$  compares diffusive and advective salt fluxes (Peclet number) and  $\xi$  is a geometric shape factor.

The solution for this problem was evaluated analytically by Henry for:  $a = 0.263$ ,  $b = 0.1$  and  $\xi = 2$ . The values of the parameter commonly used in numerical simulations are listed in Table 2.1.

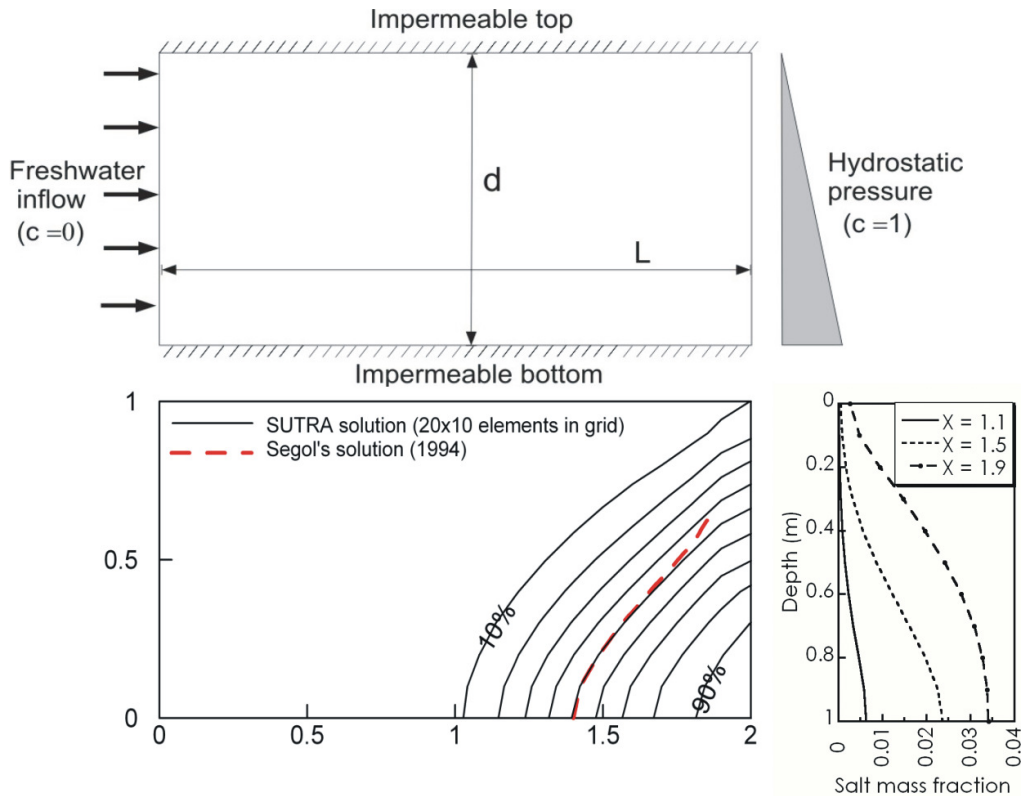


Figure 2.1: Henry problem domain and boundary conditions, *Henry* (1964). Numerical solution in terms of the concentration distribution and some vertical salinity profiles calculated at  $x = 1.1$ , 1.5 and 1.9

The history of the solution to the Henry problem is long (see *Segol* (1994) for a review). Being the only (semi-)analytical solution for boundary conditions resembling seawater intrusion it became a classic benchmark test case (*Pinder and Cooper*, 1970; *Segol et al.*, 1975; *Frind*, 1982; *Huyakorn et al.*, 1987; *Voss and Souza*, 1987; *Segol*, 1994; *Croucher and O'Sullivan*, 1995).

Table 2.1: Original parameters used in Henry problem

Parameter	Value	
$L$	$2\text{ m}$	Domain length
$d$	$1\text{ m}$	Domain thickness
$\phi$	$0.35$	Porosity
$K$	$1.0\text{E-}2\text{ m/s}$	Hydraulic conductivity (isotropic)
$D_m$	$1.88571\text{E-}5\text{ m}^2/\text{s}$	Molecular diffusion coefficient
$q_b$	$6.6\text{E-}5\text{ m/s}$	Inland freshwater flux
$\omega_0$	$0.0\text{ kg/kg}$	Mass fraction of freshwater
$\omega_s$	$0.0357\text{ kg/kg}$	Mass fraction of seawater
$\rho_0$	$1000.\text{ kg/m}^3$	Freshwater density
$\rho_s$	$1025.\text{ kg/m}^3$	Seawater density
$\epsilon$	$0.025$	Density contrast parameter $(\rho_s - \rho_0)/\rho_0$
$\mu$	$0.001\text{ kg/ms}$	Fluid viscosity

However, there are some aspects that make the problem controversial when comparing model results against the semi-analytical solution. Discrepancies have been found in the way different authors represented Henry's original problem leading to differences in the results. Most of these discrepancies, as discussed by *Croucher and O'Sullivan (1995)* and *Bues and Oltean (2000)*, are outlined below because they help in gaining insight about the problem and in motivating our work.

- Inland boundary condition.

Henry's original problem was defined in terms of stream functions. He prescribed the gradient of the stream function to be parallel to the vertical boundaries (i.e., constant unknown freshwater head along the vertical). The difference between the specified values of stream functions at the top and bottom boundaries is the total inflow integrated over a vertical cross section of the flow domain. Effectively, this implies imposing a constant but unknown head along the vertical and a fixed total flow rate. This BC is difficult to represent in conventional codes, and so it is usually substituted by a either prescribed freshwater inflow equally distributed along the vertical or a prescribed head. Probably, neither option represents accurately field conditions, where flux would be expected to be smaller and head larger at depth than near the surface. Yet, differences should be small.

- Seaside boundary condition.

Three different types of transport BC have been used to represent the contact with seawater. The first one, used by *Henry* (1964), consists of specifying seawater concentration along the whole seaside boundary. It leads to unrealistic concentrations at shallow depths, where freshwater discharge should wash out saltwater. To overcome this problem *Huyakorn et al.* (1987) divided the boundary into two parts: prescribed freshwater concentration in the 20% top portion to represent the discharge zone and prescribed seawater concentration in the rest. This boundary condition has become quite widely used but it prescribes the lower limit for outflowing freshwater without knowing a priori where the change in the flow direction takes place. Unfortunately, the actual location of this point is very sensitive to changes in flow parameters and needs to be quantified anew whenever any parameter is modified. Furthermore, the validity of this BC is questionable, as in reality there is no sharp interface between freshwater and saltwater but a transition zone. A third and more realistic BC (*Voss and Souza*, 1987; *Frind*, 1982) does not specify concentration but salt mass flux along the seaside boundary, so that whenever water enters the aquifer it carries salt concentration of seawater, but water leaving the system carries out the concentration calculated by the model at that particular location. In any case, numerical calculations show that the choice of BC has a moderate impact on the overall concentration distribution.

- Value of the diffusion coefficient ( $b$  dimensionless parameter).

*Henry* (1964) expressed the transport equation in terms of fluid velocity and a constant value for the dispersion coefficient. Porosity was not present in his equations. Some authors (*Frind*, 1982; *Huyakorn et al.*, 1987) considered the transport equation expressed in terms of Darcy's flux and used the same value of the dispersion coefficient as Henry. As a consequence, they effectively used a smaller diffusion coefficient, so that their results are not directly comparable. Diffusion opposes intrusion by producing mixing of fresh and saltwater, thus reducing the effect of buoyancy forces. Therefore, this inconsistency can be very relevant.

- Stationarity of the simulations.



Henry's solution is steady state. However, most codes solve the problem as the limit case of a transient analysis. Actually, some authors choose to fix a time of 100 minutes in their numerical simulations. However, the characteristic time of the problem is larger than 100 minutes (*Frind*, 1982) and so, an aquifer initially filled with freshwater would need much more than 100 minutes to reach steady-state conditions. As a consequence, many of the less recent numerical simulations available in the literature have not really reached steady state, and are not comparable to the existing analytical solutions.

## 2.2 Limitations of the Henry problem

The suitability of the Henry problem both as a paradigm for seawater intrusion and as a benchmarking test for density dependent codes can be questioned. Regarding the later, *Simpson and Clement* (2003) found that the concentration distribution for the uncoupled problem (density variations disregarded within the aquifer but not in the boundaries) displays a pattern similar to that of the fully coupled problem because of the strong influence of the seaside boundary condition, which makes the problem somewhat irrelevant for benchmarking. Some modifications on the values of the parameters in Table 2.1 have been proposed to improve the worthiness of the Henry problem as a benchmark test (*Simpson and Clement*, 2004). However, one of the most disturbing drawbacks of the Henry problem is that computed concentration isolines do not resemble those observed in real coastal aquifers (Figure 2.1). To illustrate this point, a review of measured salinity profiles as published in seawater intrusion literature was performed. They are shown in Figure 2.2. They look dramatically different to those resulting from the Henry problem (Figure 2.1). Salinity profiles are usually obtained by measuring the variation of electrical conductivity and temperature profiles with depth in open boreholes. It has been pointed out that these measurements are very sensitive to vertical flows that can disturb the salinity profile and produce step-like shape logs (*Custodio*, 1994). However, sharp fronts are observed even when pore water is sampled directly (Figure 2.2a). Moreover, even if the shape of the profile is disturbed by the borehole, the fact

remains that nearly 100% seawater salinity is frequently, though not always, observed at some depth, which cannot be explained by the original Henry problem. Therefore, we conclude that it is not a good representation of seawater intrusion. The above difficulty may be attributed to the fact that a large constant diffusion has been used to represent mixing. The value of the diffusion coefficient originally used by Henry is large (large value of the dimensionless parameter  $b$ ) because the solution method would have failed to converge for values of  $b$  closer to field values. As a result, it is not adequate for simulating narrow mixing layers at the interface between saltwater and freshwater (Voss and Souza, 1987). Several studies have accounted for variable dispersion to simulate the seawater intrusion in this benchmark problem (Frind, 1982; Huyakorn et al., 1987; Galeati et al., 1992; Bues and Oltean, 2000; Benson et al., 1998). They found concentration profiles similar to those of Figure 2.2, but used spherical or nearly spherical dispersion tensors (longitudinal and transverse dispersion equal or nearly so). It is clear that more realistic dispersion values need to be analyzed. Bues and Oltean (2000), who studied the advance of the diffusive and dispersive interface for  $b=0.035$  and  $0.1$ , explicitly expressed the regret on the lack of analysis of the effect of different dispersion values.

Anisotropy is another important characteristic of real aquifers which the Henry problem does not account for. Anisotropy in hydraulic conductivity may affect both seawater penetration and the flux of saltwater that enters the aquifer through the seaside boundary. Calibration results of a density dependent flow model of the transition zone in a layered basalt aquifer in Oahu, Hawaii (Souza and Voss, 1987) showed that the best fitting models were those that had an horizontal hydraulic conductivity significantly larger than the vertical one. The relevance of anisotropy in the hydraulic conductivity in coastal aquifers has been addressed frequently in the literature. However, most studies have used the sharp interface approximation in layered aquifers (Sa da Costa and Wilson, 1979; Shapiro et al., 1983; Essaid, 1990; Pistiner and Shapiro, 1993). Rumer and Shiau (1968) studied the effect of varying the ratio of horizontal to vertical hydraulic conductivity in an infinitely deep aquifer. They found that the interface becomes less steep as this ratio increases. Dispersion in anisotropic aquifers has also been considered by Reilly (1990), who pointed out the

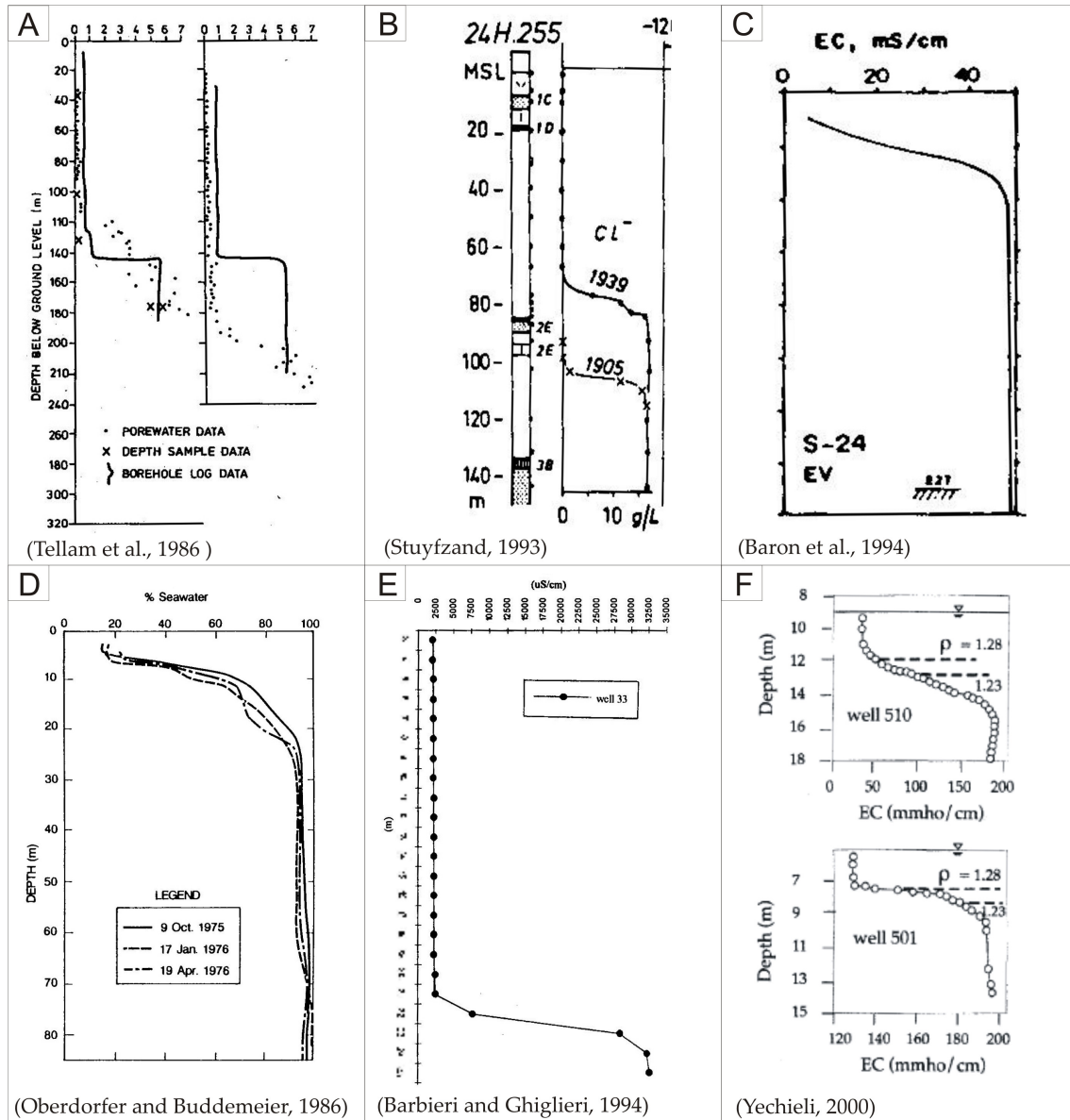


Figure 2.2: Vertical electrical conductivity profiles and vertical salinity profiles in different aquifer formations: (A) Sandstone aquifers in the Lower Mersey Basin *Tellam et al.* (1986); (B) western Netherlands *Stuyfzand* (1993); (C) carbonate aquifer in Mallorca Island, Spain *Barón et al.* (1994); (D) Enjebi Island, Enewetak coral atoll, Marshall Island, Pacific Ocean *Oberdorfer and Buddemeier* (1986); (E) alluvial aquifer in the river Foxi Baxin, Sardinia, Italy *Barbieri and Ghiglieri* (1994); (F) Dead sea area *Yechieli* (2000). Note that Dead Sea density is about  $1230 \text{ kg/m}^3$ . Notice that, while concentration is often constant below the mixing zone, its value is not always equal to that of seawater (cases A, B and E).

need of a flow-direction-dependent dispersion formulation to properly study this effect.

The objective of this work is to present a more generic description of the seawater intrusion problem exemplified by the Henry problem that includes both velocity dependent dispersion and anisotropy in hydraulic conductivity. A dimensionless analysis of the problem is carried out taking into account these additional parameters. A numerical analysis with the SUTRA code (*Voss and Provost, 2002*) is performed to assess the importance of the different dimensionless parameters in three very distinct quantities that summarize the overall behavior of the system: (1) the interface penetration, (2) the width of the freshwater-saltwater transition zone, and (3) the saltwater that flows into the system through the seaside boundary. The first two indicators are commonly used to describe the transition zone. The third indicator is of interest for reactive transport processes in the mixing zone (*Sanford and Konikow, 1989; Corbella et al., 2003; Rezaei et al., 2005*), as the reactions that take place are determined by the amount of saltwater that flows into the transition zone and mixes with freshwater. This latter variable has been usually disregarded in seawater intrusion studies, although, it was recently analyzed by *Smith (2004)*.

## 2.3 Methodology

### 2.3.1 Problem definition

A vertical cross section of a coastal aquifer is considered. Fluid flow is governed by Darcy's law, (e.g., *Bear (1972)*), which reads in terms of the equivalent freshwater head  $h$  as,

$$\mathbf{q} = -\mathbf{K} \left( \nabla h + \mathbf{e}_z \frac{\rho - \rho_0}{\rho_0} \right) \quad (2.2)$$

where  $\mathbf{q}$  is specific discharge;  $\mathbf{K}$  the freshwater conductivity tensor, which we assume diagonal with components  $K_x$  and  $K_z$ ;  $\rho_0$  the freshwater density and  $\rho$  the salt concentration dependent fluid density;  $\mathbf{e}_z$  is the unit vector in the  $z$ -direction.

Mass continuity of the fluid in steady state and in the absence of sources and sinks is given by,

$$\nabla \cdot \{\rho \mathbf{q}\} = 0. \quad (2.3)$$

Fluid density depends on salt concentration  $c$ ,  $\rho = \rho(c)$ , so that, a constitutive equation is needed.

Here we adopt a linear dependence of the fluid density on  $c$ ,

$$\rho = \rho_0 \left(1 + \epsilon \frac{c}{c_s}\right), \quad (2.4)$$

where  $\epsilon = (\rho_s - \rho_0)/\rho_0$ , and  $c_s$  is the salt concentration in seawater. Alternative approaches are suggested in the literature for cases where the contrast in densities is larger. Equation (2.3) is solved using Darcy's law (2.2) and the constitutive relationship (2.4), with the boundary conditions of specified flux ( $q_b$ ) at the inland boundary ( $x = 0$ ) and imposing  $q_z = 0|_{z=0,d}$  at both the upper and bottom impermeable boundaries. At the seaside boundary, the seawater's equivalent freshwater head is specified:

$$h|_{x=L} = d + \epsilon(d - z) \quad (2.5)$$

as illustrated in Figure 2.1.

Salt transport is described by the steady state advection-dispersion equation (e.g., *Bear (1972)*),

$$\mathbf{q} \cdot \nabla c - \nabla \cdot (\mathbf{D} + \phi D_m \mathbf{I}) \nabla c = 0. \quad (2.6)$$

where  $\phi$  is porosity,  $D_m$  is the molecular diffusion coefficient,  $\mathbf{I}$  is the identity matrix. The dispersion tensor  $\mathbf{D}$  is defined by

$$D_{xx} = \alpha_L \frac{q_x^2}{|q|} + \alpha_T \frac{q_z^2}{|q|} \quad (2.7)$$

$$D_{zz} = \alpha_T \frac{q_x^2}{|q|} + \alpha_L \frac{q_z^2}{|q|} \quad (2.8)$$

$$D_{xz} = D_{zx} = (\alpha_L - \alpha_T) \frac{q_x q_z}{|q|} \quad (2.9)$$

where  $\alpha_L$  and  $\alpha_T$  are the longitudinal and transverse dispersivity coefficients, respectively. Salt concentration  $c$  is subject to the corresponding boundary conditions. Salt mass flux across the boundary is zero at the freshwater and horizontal boundaries. At the sea boundary, we prescribe the salt mass flux according to

$$(\mathbf{q}c|_{x=L} - (\mathbf{D} + \phi D_m \mathbf{I}) \cdot \nabla c|_{x=L}) \cdot \mathbf{n} = \begin{cases} \mathbf{q}_x c|_{x=L} & \text{if } q_x > 0 \\ \mathbf{q}_x c_s & \text{if } q_x < 0 \end{cases}, \quad (2.10)$$

where  $\mathbf{n}$  is normal to the boundary pointing outwards. Fluid enters the aquifer with seawater concentration but exits with aquifer's concentration.

### 2.3.2 Dimensionless form of the governing equations

We rewrite the governing equations in dimensionless form using, when possible, Henry's dimensionless parameters. We define the dimensionless coordinates  $(x', z')$  and the ratio  $\xi$  by

$$x' = \frac{x}{d} \quad z' = \frac{z}{d} \quad \xi = \frac{L}{d} \quad (2.11)$$

Darcy's velocity, freshwater head and salt concentration are written in dimensionless form as:

$$\mathbf{q}' = \frac{\mathbf{q}}{q_b} \quad h' = \frac{h K_x}{q_b d} \quad c' = \frac{c}{c_s}. \quad (2.12)$$

With these definitions, Darcy's law reads as

$$q'_x = -\frac{\partial h'}{\partial x'} \quad (2.13)$$

$$q'_z = -r_K \frac{\partial h'}{\partial z'} - \frac{1}{a} c', \quad (2.14)$$

where

$$a = \frac{q_b}{\epsilon K_z} \quad r_K = \frac{K_z}{K_x}. \quad (2.15)$$

Here,  $r_K$  denotes the hydraulic conductivity anisotropy ratio, and  $a$  compares the freshwater influx,  $q_b$  to the characteristic buoyancy flux,  $\epsilon K_z$ . For isotropic hydraulic conductivity (i.e.,  $r_K = 1$ ),  $a$  is identical to the corresponding number defined by *Henry* (1964).

Substituting 2.13, 2.14 into 2.3, while using 2.11 and 2.12 leads to the dimensionless form of the flow equation:

$$\frac{\partial^2 h'}{\partial x'^2} + r_K \frac{\partial^2 h'}{\partial z'^2} + \frac{1}{a} \frac{\partial c'}{\partial z'} = \frac{\mathbf{q}' \cdot \nabla' c'}{1 + \epsilon c'} \quad (2.16)$$

where  $\nabla'$  indicates that the operator is written in the dimensionless distance coordinates.

The boundary conditions become:

$$\frac{\partial h'}{\partial x'} \Big|_{x'=0} = -1 \quad h' \Big|_{x'=\xi} = \frac{1}{a r_K} (1 - z') \quad q'_z \Big|_{z'=0,1} = 0. \quad (2.17)$$

Similarly, the dimensionless form of the transport equation (2.6) becomes

$$\mathbf{q}' \cdot \nabla' c' - \nabla' ((b_L \mathbf{D}' + b_m \mathbf{I}) \nabla' c') = 0 \quad (2.18)$$

where dispersion is written in dimensionless form using Peclet numbers

$$b_m = \frac{\phi D_m}{d q_b} \quad b_L = \frac{\alpha_L}{d} \quad (2.19)$$

and the dimensionless dispersion coefficients,

$$D'_{xx} = \frac{q_x'^2}{|q'|} + r_\alpha \frac{q_z'^2}{|q'|} \quad (2.20)$$

$$D'_{zz} = r_\alpha \frac{q_x'^2}{|q'|} + \frac{q_z'^2}{|q'|} \quad (2.21)$$

$$D'_{xz} = D'_{zx} = (1 - r_\alpha) \frac{q_x' q_z'}{|q'|}, \quad (2.22)$$

with

$$r_\alpha = \frac{\alpha_T}{\alpha_L} \quad (2.23)$$

Note that other expressions could have been chosen instead of  $b_L$  such as  $b_T = \alpha_T/d$  or  $b_G = \sqrt{\alpha_L \alpha_T}/d$ . However, as the effect of these dispersion coefficients is not evident *a priori*, we have chosen  $b_L$  and  $r_\alpha$  as dimensionless parameters.

The dimensionless mass flux perpendicular to the impermeable top and bottom and the fresh-water boundaries is zero.

At the seaside the transport boundary condition is given by

$$\mathbf{q}' c'|_{x'=\xi} - ((b_L \mathbf{D}' + b_m \mathbf{I}) \cdot \nabla' c'|_{x'=\xi}) \cdot \mathbf{n} = \begin{cases} \mathbf{q}' c'|_{x'=\xi} & \text{if } q'_x > 0 \\ \mathbf{q}' & \text{if } q'_x < 0 \end{cases}, \quad (2.24)$$

Thus, it turns out that the proposed problem can be written in equivalent terms to Henry's dimensionless parameters,  $a$ ,  $\xi$  and  $b_m$  and three additional numbers  $r_K$ , which is needed to account for anisotropy in the hydraulic conductivity, and  $b_L$  and  $r_\alpha$ , which account for velocity dependent dispersion. Notice that the flow equation (2.16) depends explicitly on  $\epsilon$ , which can be considered a model parameter (as it changes depending on the simulated salt and the reference concentration  $c_s$ , for example). In such a case one might wish to consider a different set of dimensionless variables. We prefer to use the dimensionless parameters as defined above to be consistent with the ones



chosen by *Henry* (1964). In the context of seawater intrusion  $\epsilon$  is small and the right side of (2.16) is of subleading order, which is reflected by the frequently employed Oberbeck-Boussinesq approximation. If  $\epsilon$  is considered a model parameter, the above choice of dimensionless parameters is still valid in the sense that no additional dimensionless parameters are required. Nevertheless,  $a$  and  $c'$  would need to be redefined as  $a = q_b/\epsilon_R K_z$  and  $c' = \epsilon c/\epsilon_R c_s$ , where  $\epsilon_R$  is a reference coefficient depending on the type of salt. Since we will only consider seawater, we take  $\epsilon_R = \epsilon$  as that of seawater, and we do not vary this parameter in our analysis.

### 2.3.3 Case definition

In order to compare the diffusive and dispersive cases, a set of dimensionless parameters have been chosen to describe the reference case. The longitudinal dispersivity coefficient used for the dispersive case is chosen so that  $b_L$  is equal to Henry's original  $b_m$  value. The reference cases used in this study and the corresponding values of dimensionless parameters are shown in Table 2.2. Note that the  $a$  value is not exactly the one used by Henry in his original calculations because the permeability tensor is anisotropic. Here,  $k_x$  and  $k_z$  are chosen so that their geometric mean is equal to Henry's original conductivity value.  $k_z$  appears in the dimensionless  $a$  parameter and it is not equal to the value of the isotropic conductivity used by Henry. The  $\xi$  factor used for these reference cases is 2.

Table 2.2: Dimensionless parameters for reference cases

CASE	$a$	$r_K$	$b_m$	$b_L$	$r_\alpha$
Diffusive	0.3214	0.66	0.1	0	0
Dispersive	0.3214	0.66	0	0.1	0.1

Besides those two reference cases presented above, different sets of simulations have been carried out varying separately each of the parameters values each time to assess their effect. Thus,  $a$  was

varied between 0.05 and 1.60;  $r_K$  ranged between 0.1 and 8;  $b_L$  between 0.01 and 1 and  $r_\alpha$  ranged between 0.04 and 5. Additional runs were performed by varying simultaneously several parameters with respect to the base-case in order to study synergic effects. In all, a total of 152 cases (92 dispersive and 60 diffusive) were run. Some of them would be unusual for field conditions (e.g.,  $r_\alpha > 1$  or  $r_K < 1$ ). Yet, we run them to explore the role of each parameter. On the other hand, most typical field conditions are covered by the adopted parameter ranges. The only exception may be the permeability anisotropy (it is not unusual to find  $r_K \ll 0.01$ ). Yet, smaller ratios led to extremely elongated intrusion wedges that might have produced numerical dispersion. In fact, the smallest ratios required elongating the model domain to avoid boundary effects. The resulting  $\xi$  factors used in the simulations were 2, 4, 8 and 16. That is, we assume that in reality  $\xi$  is very large, so that the values chosen for modelling should not affect the solution.

#### 2.3.4 Numerical analysis

The proposed problem is studied in a numerical framework. The finite element code SUTRA (Voss and Provost, 2002) was used for the simulations. The code is based on the Galerkin finite element method with quadrilateral elements. Implicit finite differences are used for the time integration. The iterative methods chosen to solve the linear system of equations are the conjugate gradient method for the flow equation and GMRES for the transport equation. Picard's method is used to solve the non-linear system.

The grid used for all simulation with  $\xi = 2$  was regular with 256x128 elements. The stability of the solution with the grid spacing was tested with grids of 200x100 and 400x200 elements, obtaining the same result in all cases. However, the 256x128 grid was chosen to be in the safe side when modifying parameters to perform the sensitivity analysis. Other studies performed with this shape factor (Oswald, 1999) showed that the results of different numerical diffusive solutions show no significant discrepancies for grid Peclet numbers below 1. Benson *et al.* (1998) studied numerical dispersion in this type of problem diffusive and dispersive form) using SUTRA and

found out that the solution was stable for grid spacing smaller than 4 cm. The grid was modified with increasing  $\xi$  as indicated in Table 2.3

Table 2.3: Number of elements used depending in the shape factor  $\xi$

$\xi$	grid elements
2	256x128
4, 8	512x128
16	768x128

### 2.3.5 Variables of interest

Seawater intrusion studies are usually concerned with the depth of inland penetration of saltwater as this characterizes the size of the contaminated zone. Therefore we will first examine the interface penetration as measured by the toe. Second, as illustrated in Figure 2.2, actual seawater intrusion is characterized by a well defined, relatively narrow mixing zone. Examining what controls their width may help in understanding field observations. Finally, though rarely examined in seawater intrusion problems, the saltwater flux is important in controlling geochemical processes in the mixing zone (*Sanford and Konikow, 1989; Rezaei et al., 2005*). In short, we analyze model results with the proposed problem in terms of the following parameters:

- $L_D = L_{toe}/d$  (Dimensionless Toe Penetration)  $L_{toe}$  is the penetration of the seawater intrusion wedge measured as the distance between the seaside boundary and the point where the 50% mixing isoline intersects the aquifer bottom (see Figure 2.3)
- $W_D$  (Dimensionless Averaged Width of the Mixing Zone) is computed by averaging  $WMZ/d$ , where  $WMZ$  is the vertical distance between isoconcentration lines of 25% and 75% mixing ratios. In order to avoid boundary effects, averaging is restricted to the interval between

$0.2L_D$  and  $0.8L_D$  (see Figure 2.3). Width was also measured along the concentration gradient, i.e. perpendicular to the interface. However, since the values obtained in both ways displayed a linear relationship, the first method was preferred because it represents better what is actually measured in the field.

- $R_D = S W M F \rho_0 / q_b c_s \rho_s d$  (Dimensionless Saltwater Flux)  $S W M F$  is the salt mass flux that enters the system across the seaside boundary (kg/s/m), evaluated using (2.24) integrated over the inflowing portion of the domain. Therefore,  $R_D$  is the ratio between the volumetric flow rates of inflowing seawater and freshwater.

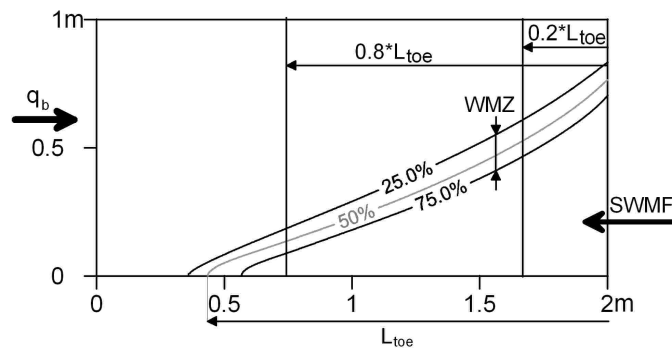


Figure 2.3: Schematic description of the variables used to quantify seawater intrusion ( $L_{toe}$ ), width of the mixing zone ( $W M F$ ) and saltwater mass flux ( $S W M F$ ).

## 2.4 Results

### 2.4.1 Diffusive versus dispersive Henry problem

The diffusive and dispersive mixing zones are shown in Figure 2.4 for the two reference cases (see Table 2.2 for the dimensionless parameters used). While the diffusive solution displays the typical broad mixing zone of the Henry problem, the dispersive solution displays the typical nearly pure seawater wedge often observed in reality.

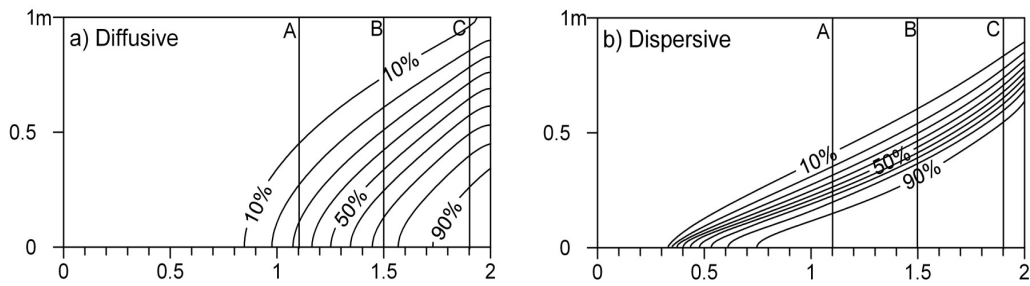


Figure 2.4: Diffusive seawater-freshwater mixing zone (a) compared to a purely dispersive mixing zone (b) for the reference cases (dimensionless parameters of Table 2.2). Notice that, contrary to the diffusive case, the purely dispersive problem displays a well defined wedge with concentration close to seawater at depth.

The difference between the diffusive and dispersive cases may be best illustrated by the vertical salinity profiles (Figure 2.5). In the diffusive profiles, salinity increases gradually and seldom reaches values near seawater concentration. The diffusive nature of Henry's original problem makes it very hard to have sections where the whole transition zone can be observed (in our plot this only happens in section C at a distance of 0.1 from the seaside boundary). On the other hand, dispersive profiles display a sharp increase in salt content, resulting in a thinner transition zone and reaching values closer to seawater concentration even for sections that are located far from the sea shore. Dispersive profiles look similar to those presented in Figure 2.2.

It must be pointed out that the poor behavior of Henry's original problem is not caused by the diffusive (i.e. velocity independent) nature of mixing. As shown in Figure 2.6, reducing the diffusion coefficient leads to concentration profiles similar to those observed in reality and obtained with dispersive mixing. This may have gone unnoticed because the influence of Henry's solution was so strong that few (*Bues and Oltean, 2000*) studied its sensitivity to  $D_m$ . In fact, both the diffusive and dispersive problems tend to Ghyben-Herzberg (static seawater, sharp front) solution as  $b$  tends to 0. Therefore, they are identical in the limit.

Solutions of the Henry problem are strongly influenced by the seaside boundary condition. This effect is so compelling that neither equivalent freshwater heads nor concentrations are dramatically changed if density dependence is ignored within the domain, as pointed out by *Simpson*

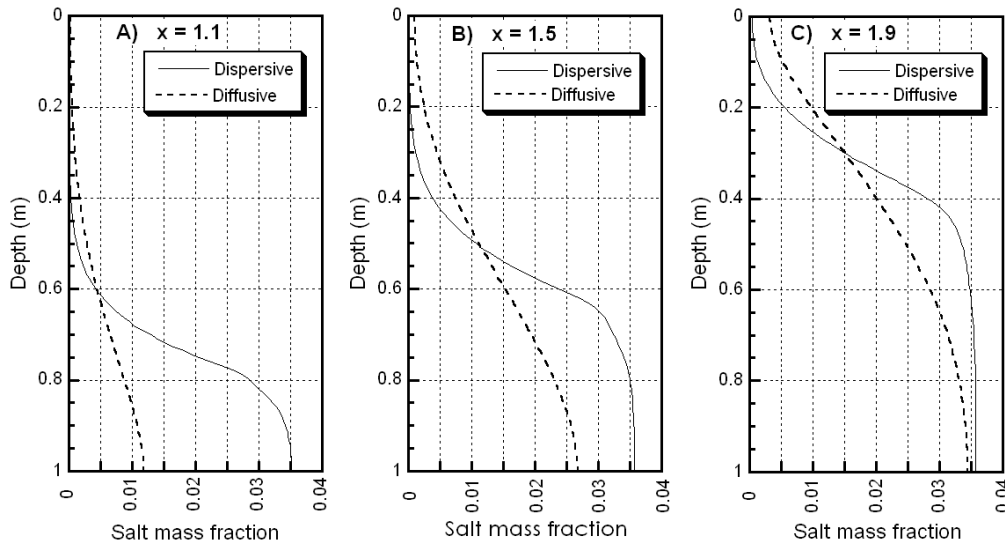


Figure 2.5: Purely diffusive and purely dispersive vertical salinity profiles located in the position indicated in Figure 2.4 at  $x = 1.1$  (A),  $1.5$  (B) and  $1.9$  (C)

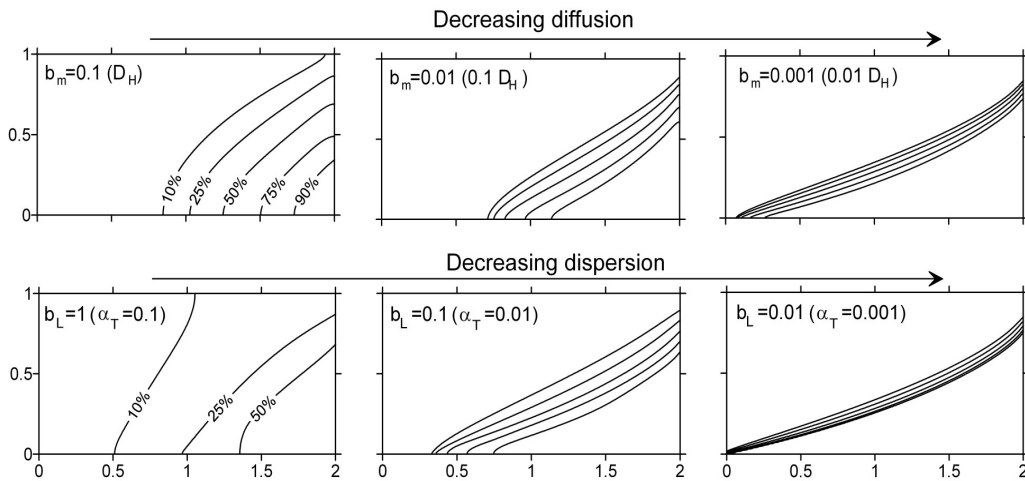


Figure 2.6: Change in the interface shape and location with increasing diffusion (upper row) and increasing dispersion (lower row).

and Clement (2003). They conclude that the traditional Henry problem is not appropriate for benchmarking and recommended to reduce the  $a$  parameter to obtain a more sensitive test for density dependent flow codes. We contend that the same effect can be obtain by reducing the Peclet number (i.e., the  $b_m$  parameter) by a factor or 10. The solutions of the resulting diffusive problem with reduced diffusion or the dispersive problem are suited for benchmarking because the

solution is indeed sensitive to density dependence within the flow domain. This is illustrated, for the dispersive case, in Figure 2.7, which displays equivalent freshwater heads and concentrations isolines for the uncoupled and fully coupled dispersive Henry problems. Differences in the results are obvious for the flow solution as well as for the concentration distribution. A similar result is obtained for a reduced diffusion problem.

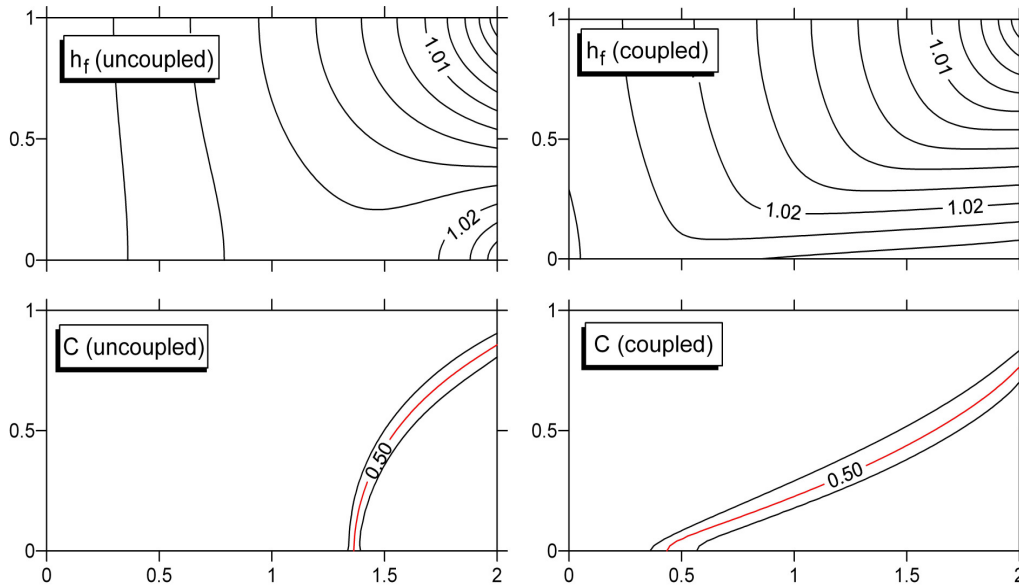


Figure 2.7: Equivalent freshwater heads ( $h_f$ ) and concentration distributions ( $c$ ) for the uncoupled (i.e. ignoring density variability within the domain) and coupled (i.e., acknowledging concentration dependence of density) dispersive Henry problem. In both cases, the downward increase of the equivalent freshwater head at the seaside boundary is sufficient to drive a significant seawater wedge into the aquifer. However its shape is very different for the two cases.

#### 2.4.2 Limitations of the dispersive Henry problem

The dispersive problem can be considered more realistic, but presents some drawbacks with respect to the original one. The first, and most important one for a benchmark test is that there is no analytical solution to compare the results against. Only comparisons between codes are possible, loosing the main strength of the Henry Problem as benchmark test. The second drawback is that numerical complexity increases. Longer transient simulations are needed to reach steady state

(Bues and Oltean, 2000). The time needed depends on the values of the dimensionless parameters chosen. For the reference dispersive case described in Table 2.2, about 1000 minutes are needed to reach steady state. It should be pointed out that this time corresponds to the time in which the 10% mixing line reaches the dynamic equilibrium. Often, the 50% line is used, which can be appropriate for evaluating the penetration of the saltwater wedge, but not for analyzing the width of the mixing zone, since the fresher side of the mixing zone takes longer than the 50% isoline to reach steady state.

The anisotropic dispersive problem is closer to reality than the original problem, however, but it is still far from reality. It does not account for relevant factors as: tidal effects, three-dimensionality, heterogeneity, transient variations of the freshwater recharge, unsaturated effects, etc. It should be viewed as a first step to understand the basics of the velocity dependent dispersion affecting seawater intrusion. Efforts are being devoted nowadays to advance further in the effect of the combination of these factors in the evolution of seawater intrusion. They should be included in the Henry problem to obtain a more realistic problem. However, simplicity to study the effect of dispersion in this type of problem would be lost.

### 2.4.3 Sensitivity to the dimensionless parameters

The shape and penetration of the saltwater intrusion wedge is controlled by the dimensionless parameters presented in Section 2. However, it is difficult to evaluate the relative importance of these parameters, especially because the dispersive problem requires more parameters than the original Henry problem. Here, we discuss the results obtained when varying the parameters with respect to the base-case, as discussed in Section 2. In order to identify, which parameter (or combination of parameters) controls each output variable, we used the DRBEST routine *IMSL MATH/LIBRARY* (1997), which uses the algorithm of *Furnival and Wilson Jr. (1974)* to identify the parameters that best explain the observed model output. The resulting regression models for each output variable ( $L_D$ ,  $W_D$  and  $R_D$ ) for the diffusive and dispersive cases are presented next.



**Toe Penetration ( $L_D$ )**

To describe the toe penetration behavior, first we have to recall the Ghyben-Herzberg (GH) approximation which consists of neglecting mixing and, hence, salt fluxes. When coupled to the Dupuit's assumption, it yields reasonable estimations of the location of the interface (see, e.g., Bakker (2006)) The toe position derived from this assumption can be expressed in terms of the dimensionless parameters defined in Section 2:

$$L_{GH_D} = \frac{L_{GH}}{d} = \frac{1}{2ar_K} \quad (2.25)$$

This expression is the limit case when diffusion ( $b_m$ ) or dispersion ( $b_L$ ) tend to 0. The toe recedes when diffusion/dispersion is increased. The deviation from  $L_{GH_D}$  is due to the head loss caused by seawater flux. Since this is driven by the diffusive/dispersive flux of salt across the mixing zone, one should expect this deviation to be sensitive to the Peclet numbers. Therefore, we should be able to express  $L_D$  as  $L_{GH}$  minus a term depending on the Peclet numbers.

The best regressions obtained are presented in Figure 2.8 for the dispersive and diffusive cases. Regressions are not perfect, especially for the dispersive case. It has to be pointed out that the existence of numerical dispersion may affect the results when dispersion is really small making impossible to find a perfect fit. Nevertheless, the regressions allows us to identify the key factors affecting the toe position. It is observed that in both problems the deviation from the Ghyben Herzberg toe position is a function of the Peclet number. The simplest combinations of model parameters to explain the deviation from the GH approximation are:

$$F_{LDS} = 0.136 \left( \frac{\alpha_G}{a_x^2 \sqrt{r_K}} \right)^{0.724} 0.69 \left( \frac{\alpha_G}{a_x^2 \sqrt{r_K}} \right)^{0.362} \quad \text{for the dispersive problem} \quad (2.26)$$

$$F_{LDF} \approx \frac{1.64 b^{\frac{1}{3}} - 1.18 b^{\frac{1}{2}}}{a_x} \quad \text{for the diffusive problem} \quad (2.27)$$

where  $a_x = a r_K = q_b / K_x \epsilon$  and  $\alpha_G = \sqrt{\alpha_L \alpha_T}$ .

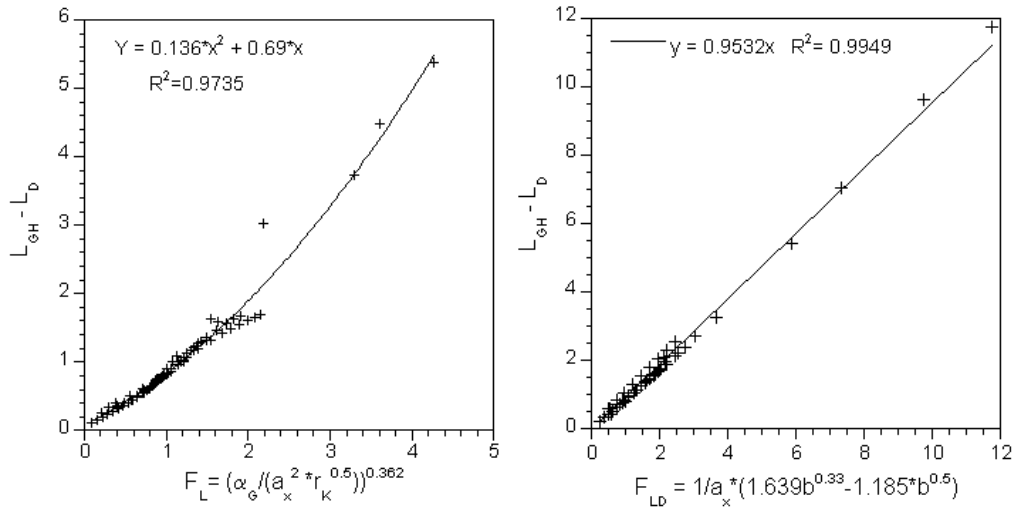


Figure 2.8: Regressions obtained for the deviation of the toe penetration with respect to the Ghyben-Herzberg toe position for the dispersive (left) and diffusive (right) case

The points that diverge from the regressions are those whose anisotropy ratio ( $r_K$ ) is smaller than 0.5. This fact indicates that the effect of a strong anisotropy is not properly characterized by these expressions. This may be a result of the disregard of anisotropy in the permeability when evaluating  $L_{GH}$ .

#### Width of the mixing zone ( $W_D$ )

The average width of the mixing zone was evaluated only for the dispersive case. As shown in Figure 2.5, the width of the mixing zone is highly dependent on  $x$  for the diffusive case, due to the high diffusion coefficient used in most diffusive simulations. Moreover, it is truncated by the upper and lower boundaries. Therefore, we do not consider it to be a representative parameter. For dispersive problems, this parameter is nearly constant for the central portion of the mixing zone except for cases with a very small seawater wedge penetration (Figure 2.9b). The width of the mixing zone has been computed between  $0.2 L_D$  and  $0.8 L_D$  to avoid the region near the toe

(Figure 2.9b).

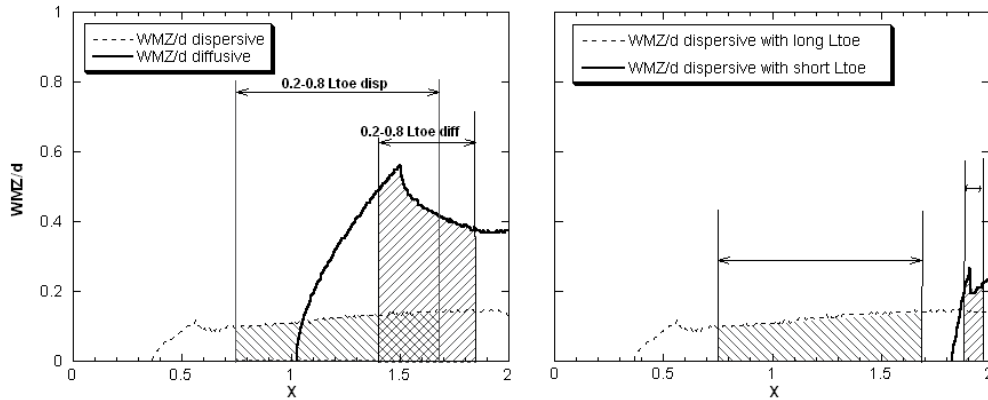


Figure 2.9: Width of the mixing zone versus  $x$  in the diffusive and dispersive reference cases. This parameter changes moderately with distance in dispersive problems, so that it can be used in the analysis. This is not the case in the diffusive problems.

The role of longitudinal and transverse dispersivity in the dispersive problem can be analyzed by examining Figure 2.10, where one can observe that water flows parallel to the concentration isolines. This velocity field suggests that transverse dispersivity controls mixing throughout most of the transition zone whereas longitudinal dispersivity is only relevant at the lowest portion. A close analysis of Figure 2.10 yields some insights on transport processes at the mixing zone. Above the 60% isoline, flux is essentially parallel to the isolines, so that most salt is carried upwards by lateral dispersion. The fact that the separation increases upwards reflects both a decrease in dispersive flux (some salt is transported along the mixing zone because water flux also increases seawards) and an increase in dispersion coefficient (in response to the increase in flux). Below the 60% isoline, water flux is small, so that both longitudinal and advection contribute also to the upwards salt flux. Overall, salt is dispersed upwards and advected sideways. As water flux and, hence, dispersion increase seawards, so does the returning salt flux, thus balancing the essentially advective but continuous flux from below the mixing zone.

The above discussion reflects that the interplay between advection and longitudinal and trans-

verse dispersion is non-trivial, even in this idealized problem. However, proper understanding is relevant because the role of transverse dispersion in solute transport is a subject of some controversy. Based on stochastic transport results, most authors argue that this parameter would tend to zero for long travel distances (*Dagan, 1989*). Yet, other authors argue that the interplay between spatial heterogeneity and time fluctuations of velocity leads to sizeable macroscopic large scale transverse dispersion (*Dentz and Carrera, 2003; Cirpka and Attinger, 2003; Dentz and Carrera, 2005*). The fact that the behavior of the mixing zone is so sensitive to transverse dispersion implies that actual detailed measurements at the mixing zone should contribute to understand field scale lateral dispersion.

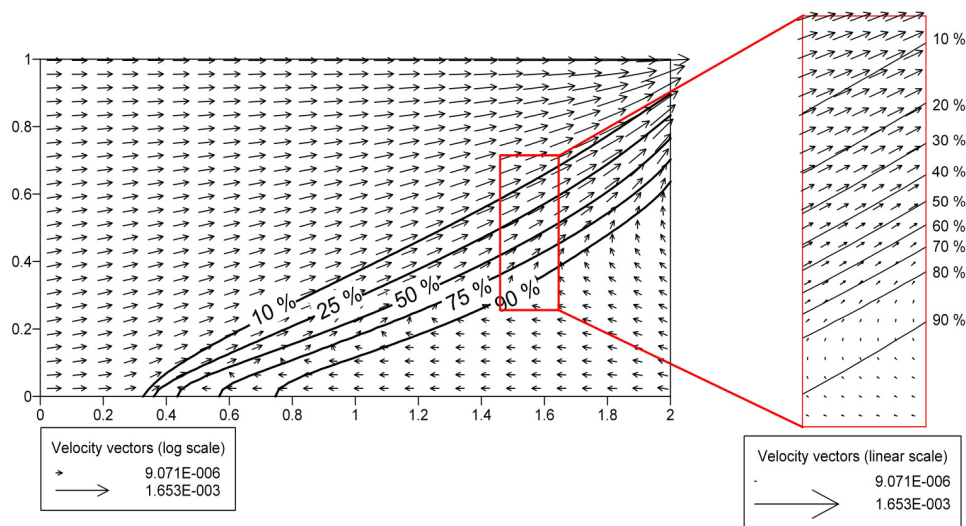


Figure 2.10: Velocity field and 25, 50 and 75% concentration isolines in the dispersive reference case.

Sensitivity of the width of the mixing zone,  $W_D$ , to the longitudinal and transverse dispersion is substantiated by Figure 2.11, which shows a linear relationship between  $W_D$  and the geometric mean of the two dispersivities. That is, transverse and longitudinal dispersivities contribute equally to the width of the mixing zone. This is somewhat disappointing because the discussion around Figure 2.10 suggest that lateral dispersion might have been the dominant one.